

Ecofriendly Synthesis of Cobalt Nanoparticles Using *Millettia pinnata* and Evaluation of Embryonic Toxicology and Anticancer Activity

Iadalin Ryntathiang¹, Devanand Gulab Chaudhary², Yagavel Pooja¹, Archana Behera¹, Yuvashree Chandrasekaran¹, Mukesh Kumar Dharmalingam Jothinathan^{1*}

¹Department of Biochemistry, Saveetha Medical College and Hospital, Saveetha Institute of Medical and Technical Sciences (SIMATS), Saveetha University, Chennai, India.

²Department of Paediatrics, Saveetha Medical College and Hospital, Saveetha Institute of Medical and Technical Sciences (SIMATS), Saveetha University, Chennai, India.

Abstract

Nanotechnology driven approaches have gained significant attention especially in biomedical research particularly in the green synthesis of metal nanoparticles offering ecofriendly and sustainable alternatives for therapeutic applications. This study explored the green synthesis of cobalt nanoparticles (CoNPs) from *Millettia pinnata* and evaluated their embryonic toxicology and anticancer activity against osteosarcoma cells. CoNPs were synthesized and characterized using UV-Vis spectrophotometry, FTIR spectroscopy and SEM-EDAX analysis. UV-Vis analysis confirmed CoNPs formation at 320 nm, while FTIR identified O-H, C=C and metal ligand vibrations. SEM showed nanoparticle agglomeration with an average size of 100 nm and EDAX confirmed cobalt and chlorine presence. The antimicrobial activity of CoNPs was assessed through time kill curve analysis against *Candida albicans*, *Klebsiella sp.*, *Enterococcus faecalis* and *Streptococcus mutans*. The results demonstrated strong efficacy against *S. mutans*, moderate activity against *Klebsiella sp.* and *E. faecalis* and low anticandidal activity against *C. albicans*. Cytotoxicity studies using MTT assays showed a dose dependent reduction in osteosarcoma cell viability, further confirmed by apoptosis detection through AO/EtBr staining. Toxicity assessments including brine shrimp lethality assays (BSLA) and zebrafish embryo tests revealed dose and time dependent effects. These findings suggest that *M. pinnata* derived CoNPs exhibit strong antimicrobial and cytotoxic properties, especially against *S. mutans* and osteosarcoma cells, warranting further research into their therapeutic potential and environmental impact.

Keywords: Antimicrobial Activity, Brine Shrimp Lethality Assays, Cobalt Nanoparticles, *Millettia pinnata*, Nanotechnology, Zebrafish.

Introduction

Nanotechnology is viewed as the next industrial revolution with significant impacts on society, the economy and the global economy. Nanotechnology has many applications in fields such as bioengineering, chemistry, biology and physics. This sector operates on the nanometer scale, providing several benefits and applications in various

scientific disciplines [1, 2]. Nanoparticles (NPs) created in various ways have gained interest due to their unique properties [3]. When examining the future use of nanomaterials, the need for green chemistry is clear. The advancement of nanoscience should result in the development of ecologically safe and sustainable nanoparticles that can be universally recognized in the field of nanotechnology [4]. Researchers use cobalt

based nanoparticles for various applications because of their chemical and physical characteristics. It has biological and cytotoxic properties, as well as superior permanent magnetic properties [5]. The green synthesis of cobalt oxide (Co₃O₄) NPs using *Ziziphus oxyphylla* Edgewood root has the potential for antibacterial applications in pharmaceutical and medical science [6]. In addition, the biosynthesis of Co₃O₄ NPs using *Hyphaene thebaica* fruit showed high photocatalytic activity. Energy dispersive X-ray spectroscopy (EDAX) was performed with Scanning Electron Microscope (SEM) to analyze the elemental composition of Co₃O₄ NPs [7]. Several functional groups present in the plant extract that act as capping and stabilizing agents were identified using Fourier transform infrared spectroscopy (FTIR) analysis [8]. UV-Vis spectroscopy was used to identify the green mediated Co₃O₄ NPs establishment from the absorbance peaks [9]. The plant species *Millettia pinnata* is widely distributed in India and is a member of the Fabaceae family. Several components of this plant are used to treat various conditions [10]. By performing the photocatalytic degradation of dyes, copper oxide nanoparticles (CuO NPs) were assessed for visible light aided photocatalytic activities. CuO NPs were produced using *M. pinnata* leaf extract by an ecologically friendly, economical, dependable and straightforward green synthesis approach [11]. A study was conducted to assess the effectiveness of green synthesized gold nanoparticles derived from *M. pinnata* in non small cell lung cancer cell lines [12]. In particular, NPs have been proven to be effective against both Gram positive and Gram negative bacteria, exhibiting broad spectrum antibacterial capabilities. According to a study, Co₃O₄ NPs are effective against gram negative (*Klebsiella pneumoniae*, *Pseudomonas aeruginosa* and *Escherichia coli*) and gram

positive (*Staphylococcus aureus*, *Staphylococcus epidermidis* and *Bacillus subtilis*) bacterial infections. These researchers discovered that as the concentration of these NPs increased, so did their antibacterial activity [13]. The antibacterial activity of biosynthesized cobalt nanoparticles (CoNPs) was seen against all types of bacteria; however, it was not as strong as that of a crude extract from onion and garlic peels [14]. Furthermore, the use of zebrafish in toxicology studies has contributed to our understanding of the possible harmful effects of NPs on living things. For instance, researchers discovered that some NPs can alter gene expression or result in defects in the development of zebrafish embryos [15]. A previous study found that CoNPs cause oxidative stress and apoptosis, which lower the expression of myogenic genes and damage zebrafish muscle tissue [16]. High CoNPs exposure levels are harmful to zebrafish embryos and hurt development [17]. CoNPs synthesized using a green synthesis method were evaluated using an MTT assay for *in vitro* cytotoxicity investigation to determine their potential anticancer applications [18]. The percentage of cell viability in the osteosarcoma cancer cell line steadily decreased with increasing concentrations of green synthesized selenium nanoparticles, according to the results of the MTT assay used in the study [19]. Thus, the study aims to analyze the green synthesis of CoNPs using *M. pinnata* and its embryonic toxicology evaluation using zebrafish and brine shrimp lethality assay (BSLA) and *in vitro* anticancer activity against osteosarcoma cells.

Materials and Methods

CoNPs are synthesized using *M. pinnata* leaf (MPL) extracts and characterized by various assays [20]. Figure 1 displays a graphical abstract of the green synthesis of CoNPs using leaf extracts.

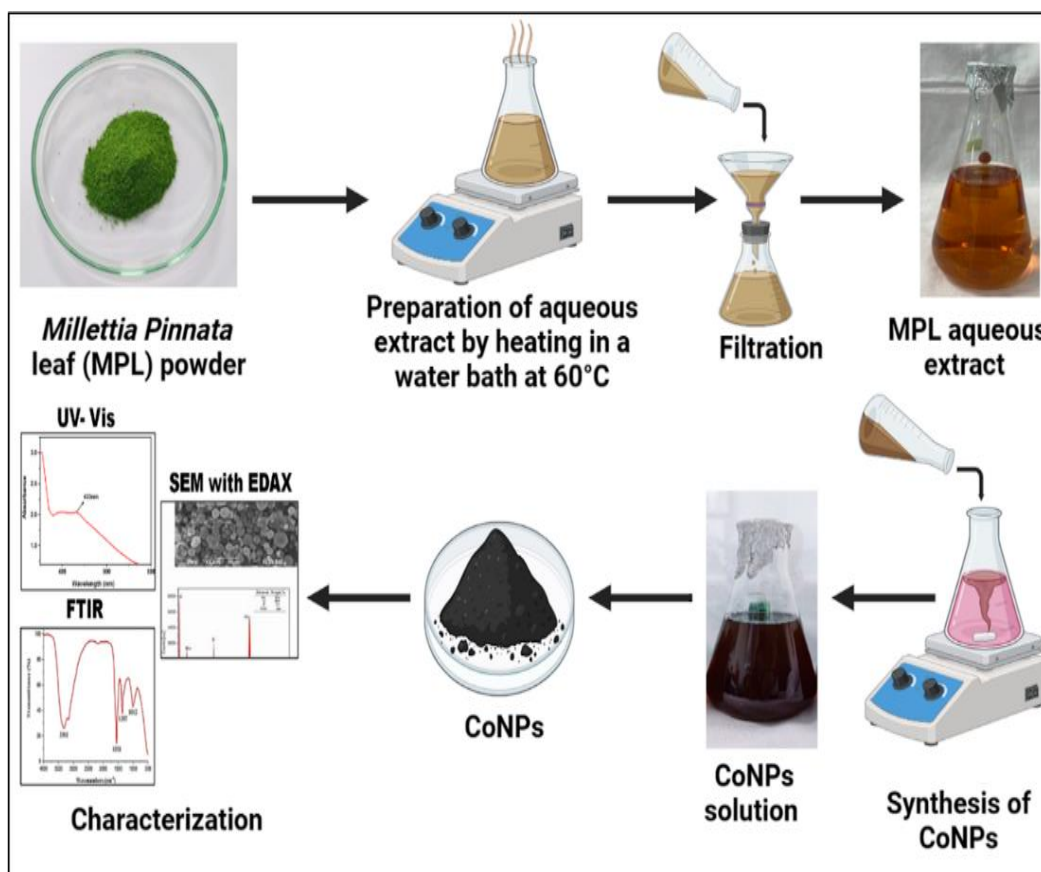


Figure 1. Graphical Abstract of Green Synthesis of Cobalt Nanoparticles Using *Millettia pinnata* Leaf Extract

Collection of Plant Sources

MPL was collected from Chennai, Tamil Nadu, India, from June to July 2023. The samples were verified by the Centre for Advanced Studies in Botany at the University of Madras, Chennai, India.

Preparation of Extracts

The MPL was chopped into small pieces, washed 3 times with tap water and subsequently air dried in a shaded area for 3 days. Once the MPL were fully dried, they were ground into a fine powder and stored for future use. Subsequently, 25 g of MPL powder was poured into a 300 mL solution of double distilled H₂O at 60°C for 20 mins. Afterwards, the extract was filtered using a muslin cloth and further refined using a Whatman filter paper with a diameter of 125 mm. The filtered solution was subsequently stored at a temperature of 4°C for further use.

Preparation of Cobalt Chloride Solution

A 5mM cobalt chloride (CoCl₂) solution was prepared by dissolving it in 300 mL of distilled water.

Synthesis of Cobalt Nanoparticles

To synthesize CoNPs, 10 mL of MPL was combined with 90 mL of a CoCl₂ solution (5 mM) and agitated at 35°C. The acidity level of the reaction mixture was consistently checked and recorded. Subsequently, the reaction mixtures were incubated in a dark room on a rotating shaker at 40°C and a speed of 300 rpm for 3 h. The visual evaluation of the reaction mixture's colour was followed by incubation at room temperature for 72 h. After the incubation period, a total colour change was detected in the reaction mixture, indicating the successful synthesis of NPs. Conversely, the control containing only CoCl₂ exhibited no colour change. Figure 2 shows a graphical abstract of the synthesized CoNPs application.

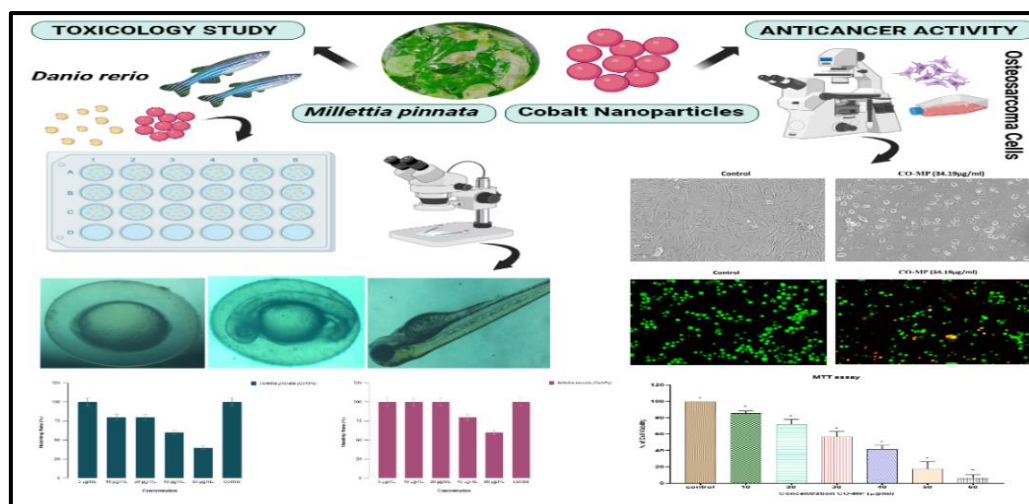


Figure 2. Graphical Abstract of Applications of Synthesized Cobalt Nanoparticles

Characterization of Cobalt Nanoparticles

The CoNPs were characterized using UV-vis spectroscopy, FTIR spectroscopy and SEM with EDAX. Synthesis was first detected using UV-visible spectrophotometry in the range of 200-800 nm. The FTIR analysis at 4000-400 cm^{-1} , successfully identified the specific functional groups present on the CoNPs. The morphology and purity were evaluated using SEM with EDAX.

Antimicrobial Activity

Antimicrobial activity was evaluated using CoNPs synthesized by MPL using the agar well diffusion method. The bacterial culture selected one gram positive (*Staphylococcus mutans*), two gram negative bacteria (*Klebsiella sp.* and *Enterococcus faecalis.*), and *Candida albicans* [21].

Time Kill Curve Analysis

To assess the bactericidal properties of CoNPs, a time kill curve was employed, following a methodology similar to that described in the author's research work [22] and their correlation with the growth patterns of the three above mentioned bacteria was analyzed. This assay involved the cultivation of these pathogens in Mueller Hinton broth with varying concentrations of CoNPs (ranging from 100 μg to 1000 μg) while tracking their growth at specified time intervals. To ensure consistent

results, preliminary growth curves were established, ensuring that the pathogens reached a stable early phase to mid log bacterial phase after a five hour pre incubation period in antibacterial free Mueller Hinton Broth. A 0.5 McFarland inoculum of each pathogen was meticulously prepared in sterile phosphate buffered saline (PBS) and derived from cultures grown on Mueller Hinton agar plates at 37 $^{\circ}\text{C}$ for 18-20 h. Subsequently, 30 μL of this inoculum was diluted in 15 mL of pre warmed (37 $^{\circ}\text{C}$) antibacterial free Mueller Hinton broth, and 90 μL of this resultant mixture was carefully dispensed into each well of a 96 well enzyme linked immunosorbent assay (ELISA) plate. To each well, 10 μL of MPL CoNPs at five different concentrations were added and an untreated control was included in the assay for reference.

Embryonic Toxicology Analysis on Cobalt Nanoparticles in Zebrafish

Zebrafish embryos were incubated in the water culture medium and were maintained at a temperature of 26 $^{\circ}\text{C}$. Embryos that were chosen at random, 4 h after fertilization (during the spherical stage), were kept in a 10 mL solution of zebrafish culture water. Viable embryos were placed on 96 well culture plates containing 0.2 mL of culture water. Then 0.1 mL of CoNPs synthesized by MPL at various concentrations (5, 10, 20, 40 and 80 $\mu\text{g}/\text{mL}$)

was applied to each well. The experiment consisted of three replicates, where the control group consisted of embryos in the culture medium. The plates were placed in an incubator set at 26°C. The developmental progress of embryos and zebrafish larvae was monitored at various time points after fertilization. The hatching and mortality rates were determined at 12 h intervals based on the number of viable embryos. The NPs were observed to cause malformations in embryos under a microscope [23].

Toxicology Study of Cobalt Nanoparticles in Brine Shrimp

The brine shrimp lethality assay (BSLA) was used to evaluate the cytotoxicity of CoNPs synthesized using MPL at different concentrations (5, 10, 20, 40 and 80 µg/mL). The assay was conducted using an approach described in prior work [24].

Cell Viability in the MTT Assay

Fibroblast cells were cultured individually in 96 well plates at a density of 5×10^3 cells per well in DMEM media supplemented with 10% FBS and 1X antibiotic solution. The cells were then placed in a CO₂ incubator at 37°C with a CO₂ concentration of 5%. The cells were rinsed with 100 µL of 1X PBS and then exposed to CoNPs. Subsequently, the cells were incubated at 37°C with 5% CO₂ for 24 h. Following the treatment, the liquid in the container was removed, and the cells were exposed to MTT (0.5 mg/mL in 1X PBS) at 37°C for 4 h. After the incubation period, the media containing MTT was removed, the cells were rinsed with 100 µL of PBS and the crystals formed were dissolved in 100 µL of DMSO. The absorbance of the generated purple blue formazan dye was quantified at 570 nm using a microplate reader. Cell vitality was determined based on a previously described approach [25].

To examine the impact of CoNPs synthesized by MPL on cell morphology, a total of 2,00,000 normal fibroblast cells were evenly

distributed in six well plates and subjected to either CoNPs treatment or no treatment for 24 h. After treatment, cells were rinsed with PBS and examined using an inverted phase contrast microscope.

Results

UV Spectra of Cobalt Nanoparticles

A UV-Vis spectrophotometer was used in the 300-600 nm range to assess the synthesis, optical properties and stability of CoNPs from *M. pinnata* leaf extract. UV-visible spectroscopy provided insights into the interaction between metal ions and bioactive compounds in the extract, showing a pronounced absorbance peak at 320 nm shown in Figure 3 with maximum absorbance close to 2.0 confirming CoNPs synthesis. This peak signifies the interaction of CoNPs with UV light, indicative of cobalt based nanoparticles and their electronic transitions. Metal nanoparticles like CoNPs absorb light through oscillating conduction band electrons, influenced by plasmon resonance, dielectric medium and nanoparticle characteristics. The sharp decrease in absorbance beyond 400 nm suggests that CoNPs are mainly UV-absorptive, with minimal absorbance in the visible spectrum, indicating small, monodispersed particles that enhance surface plasmon resonance (SPR) in the UV range.

The UV-Vis absorption plot reveals an intense band around 300-350 nm, peaking at 320 nm, followed by a low, stable absorbance in the visible to near infrared (VIS-NIR) region. This pattern highlights the nanoparticles electronic structure and potential applications. CoNPs are effective UV blocking agents, with promising uses in environmental, biomedical and industrial fields due to their optical properties, which are essential for characterizing and standardizing CoNPs for further research in nanoparticle technologies [8].

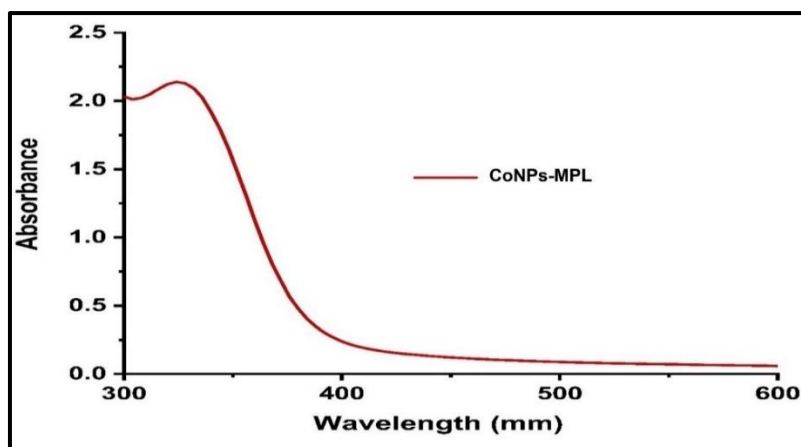


Figure 3. UV-Visible Spectra of Cobalt Nanoparticles

FTIR of Cobalt Nanoparticles

FTIR spectroscopy is extensively used to identify functional groups by analyzing characteristic wavenumbers from 4000 to 400 cm^{-1} , where the horizontal axis shows wavenumbers and the vertical axis displays % transmittance. This method is essential in natural products research, as it helps detect bioactive compounds and provides valuable information on molecular composition. In the synthesis of CoNPs from *M. pinnata* leaf extracts, FTIR was utilized to identify functional groups acting as capping and stabilizing agents. The spectrum revealed distinct peaks that correspond to various molecular vibrations, indicating specific functional groups.

From Figure 4 a noticeable peak at 3229.872 cm^{-1} signifies O-H stretching vibrations,

commonly found in alcohols, phenols and carboxylic acids, suggesting hydrogen bonding. The peak at 1608.776 cm^{-1} likely results from C=C stretching in aromatic rings or alkenes, indicating aromatic or unsaturated hydrocarbons. Peaks at 1394.840 cm^{-1} and 1040.490 cm^{-1} are attributed to C-H bending and C-O stretching vibrations, characteristic of alkanes, alcohols, ethers, esters or carboxylic acids. Lower wavenumber peaks at 497.871 cm^{-1} , 418.295 cm^{-1} and 433.855 cm^{-1} hint at metal ligand or metal oxygen vibrations, possibly indicating metal organic frameworks or complex molecular structures. The FTIR spectrum thus provides a comprehensive profile, highlighting hydrogen bonded, hydrocarbon and metal ligand interactions, reflecting a complex molecular composition of the sample [21].

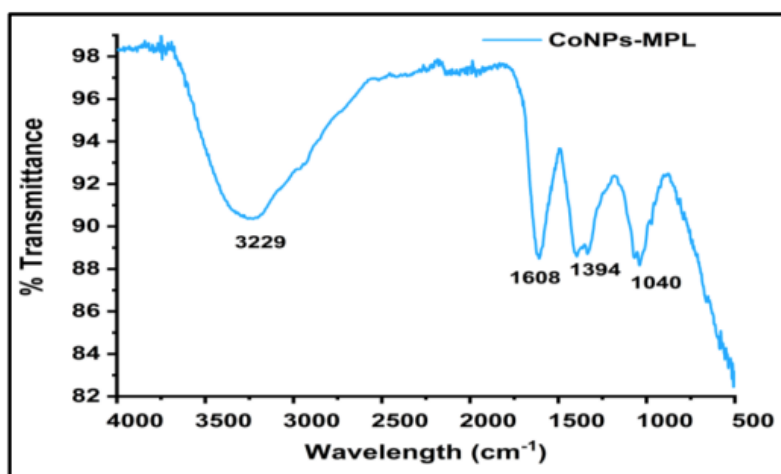


Figure 4. Fourier Transform Infrared Spectra of Cobalt Nanoparticles

SEM with EDAX

The surface morphology of *M. pinnata* CoNPs was analyzed by SEM and the results are shown in Figure 5. Particle agglomeration in this study is influenced by the chemical constituents and secondary metabolites in MPL extract, which helps encapsulate and stabilize individual nanoparticles. These functional groups promote particle attraction and reactivity, leading to the formation of larger particles. SEM images reveal that the nanoparticles tend to agglomerate, with

individual particles appearing roughly spherical or irregular in shape, indicating non uniform morphology. The particle size falls within the nanometer range (approximately 100 nm, based on the scale bar), exhibiting a broad size distribution. Some particles are notably larger. The rough surface of the nanoparticles may result from the synthesis method or the biomolecules from MPL extract, which could act as capping agents and promote agglomeration during drying or due to the intrinsic properties of the nanoparticles [8].

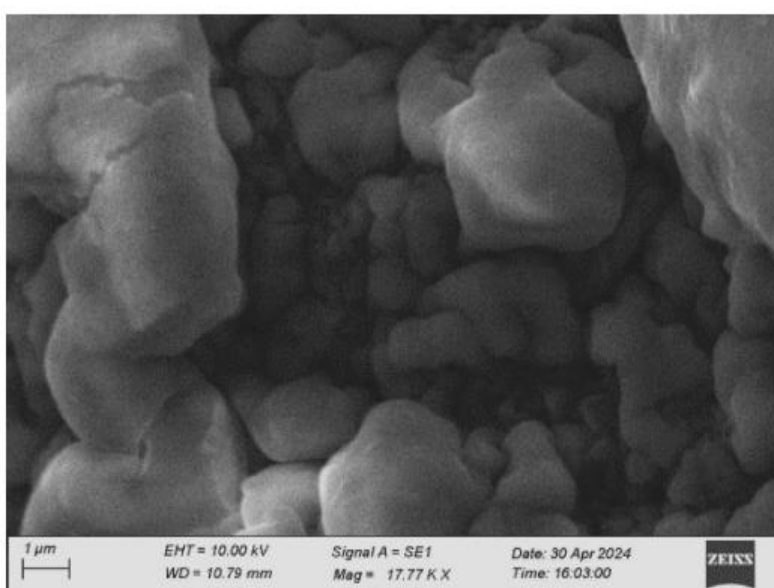


Figure 5. Scanning Electron Microscopic Image of Cobalt Nanoparticles

Figure 6 illustrates the EDAX spectrum of *M. pinnata* CoNPs, with the corresponding table displaying a quantitative elemental analysis. EDAX, an analytical technique for elemental composition, shows spectrum peaks that represent various elements in the sample. The x-axis reflects the energy of emitted X-rays, while the y-axis shows counts, indicating element concentration. Analysis within the 0–6 keV range identified key elements in the CoNPs.

The spectrum's peaks reveal a significant oxygen presence (~0.67 keV; Weight %: 27.45, Atomic %: 48.56), commonly associated with oxides or organic materials. Cobalt, with notable amounts (peaks ~0.77 and 6.92 keV;

Weight %: 21.97, Atomic %: 10.56), likely indicates a cobalt oxide compound. Sodium appears in minor quantities (~1.04 keV; Weight %: 1.74, Atomic %: 2.14), potentially as an impurity. Chlorine, with high concentration (peaks at 2.62 and 2.81 keV; Weight %: 45.36, Atomic %: 36.22), suggests the presence of chloride compounds. Potassium (~3.31 and 3.59 keV; Weight %: 3.48, Atomic %: 2.52) also appears in trace amounts. The SEM EDAX findings confirm the sample is predominantly composed of chlorine and oxygen, with significant cobalt and minor sodium and potassium, suggesting a chloride based material with potential cobalt oxides [7, 8].

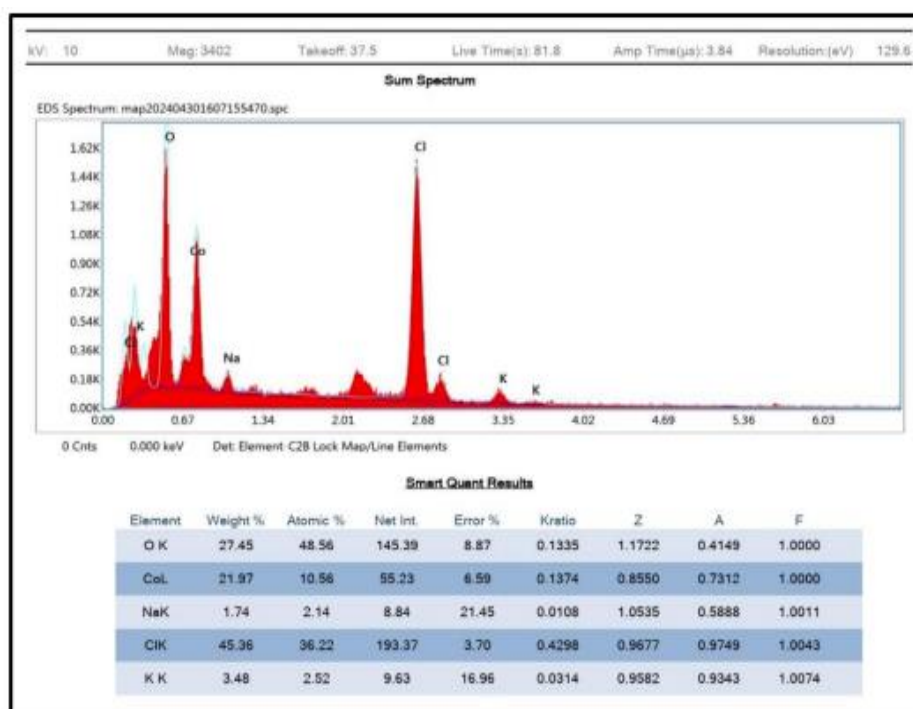


Figure 6. Scanning Electron Microscope Energy Dispersive X-ray spectra and Elemental Composition of Cobalt Nanoparticles from Leaf Extract

Antimicrobial Activity

Figure 7 shows the antimicrobial activity of *M. pinnata* CoNPs against four different microorganisms (*C. albicans*, *S. mutans*, *E. faecalis* and *Klebsiella sp.*). The clear zones around the wells indicate the inhibition of microbial growth by the NPs. The size of the inhibition zone varies depending on the microorganisms, indicating varying degrees of susceptibility to the CoNPs. The largest inhibition zone is observed against *C. albicans*, suggesting that it is the most susceptible to CoNPs. Overall, our data suggests that *M. pinnata* (CoNPs) has potential as an antimicrobial agent.

Figure 8 depicts the antimicrobial efficacy of CoNPs synthesized from *M. pinnata* leaf extract against various microorganisms, measured by the zone of inhibition (mm). The tested microorganisms include *C. albicans*, *S. mutans*, *E. faecalis* and *Klebsiella sp.*, with different CoNPs concentrations (100 µg/mL, 50 µg/mL and 25 µg/mL) and a control group. Key findings indicate that *C. albicans* exhibits a

dose dependent inhibition, with larger zones of inhibition as CoNPs concentration increases, demonstrating a strong sensitivity to CoNPs. *S. mutans* also shows dose dependent inhibition but with comparatively smaller zones, indicating moderate sensitivity. Among the microorganisms, *E. faecalis* is the least affected, with minimal increases in the inhibition zone, suggesting lower sensitivity to CoNPs. *Klebsiella sp.*, however, shows some inhibition in the control group, implying an inherent antimicrobial effect from the control, which is further amplified by CoNPs in a dose dependent manner.

Overall, increasing CoNPs concentrations enhances bacteriostatic effects across all organisms. *Klebsiella sp.* and *C. albicans* are the most sensitive, followed by *S. mutans* with moderate sensitivity and *E. faecalis* being the least sensitive. These findings highlight the potential of *M. pinnata* CoNPs as antimicrobial agents, particularly against *C. albicans*, *Klebsiella sp.* and *S. mutans*, while further studies are needed to clarify their mechanisms, safety and therapeutic applications [8].

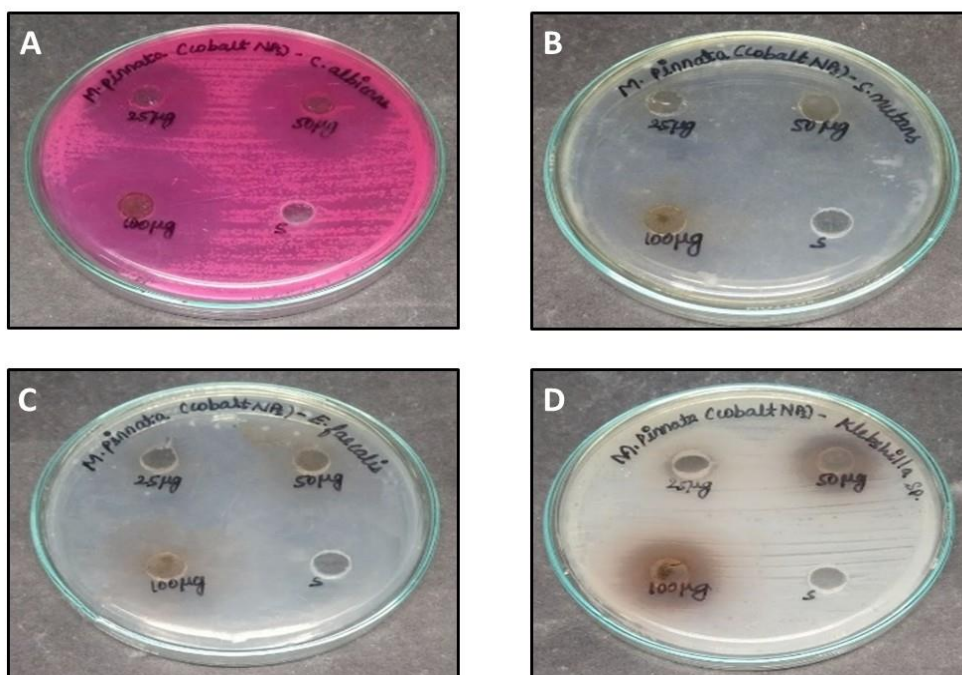


Figure 7. Zone of Inhibition of Cobalt Nanoparticles Against (A) *C. albicans*, (B) *S. mutans*, (C) *E. faecalis*, (D) *Klebsiella sp*

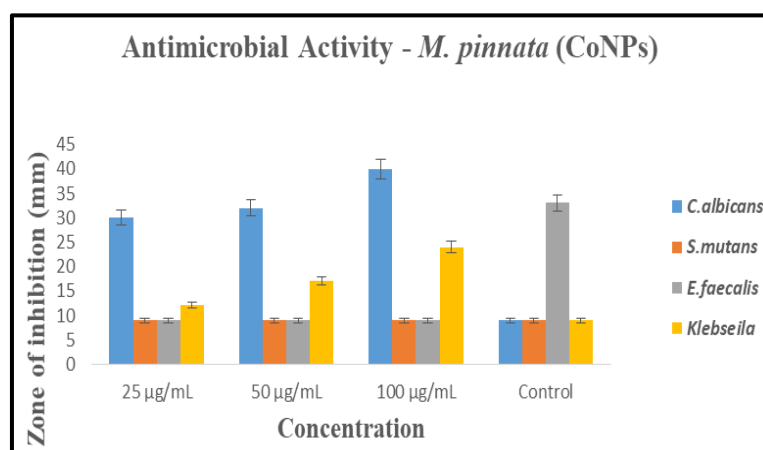


Figure 8. Antimicrobial Activity of Cobalt Nanoparticles

Time Kill Curve Analysis of Cobalt Nanoparticles

A time kill assay is a marker that is used to measure the effectiveness of an antimicrobial agent in a given period. It determines the number of minutes taken by a particular substance to kill a particular microorganism. This test is commonly carried out by incubating the microorganism at a fixed concentration with the substance and then quantifying the number of viable cells at predetermined intervals. Figure 9 is a graphical representation of the time kill assays done on CoNPs extracted from

MPL with the following microorganisms; *C. albicans*, *Klebsiella sp.*, *E. faecalis* and *S. mutans*. In both graphs, the horizontal axis represents time in hours and the vertical axis represents the logarithm of colony forming units per millilitre (log CFU/mL). Various lines signify varying CoNPs concentrations; a standard antibiotic and a control group, which contains no CoNPs are presented for comparison.

Notably, CoNPs possess low anticandidal activity against *C. albicans*. The above findings signify that CoNPs exhibit low antifungal

efficacy against *C. albicans*. This shows that the CFU/mL does not differ substantially when compared to the start time, suggesting that the CoNPs do not affect decreasing the number of viable cells at all tested concentrations. The control group and the CoNPs treated groups are generalizable, indicating a lack of strong inhibitory effects. In *Klebsiella sp.*, the CoNPs exhibit some antibacterial activity. At higher concentrations (50 and 100 µg/mL), the CFU/mL was slightly reduced over some time which shows that there is some bacterial inhibition. However, the decrease was not as significant as that of standard antibiotics, which indicates that the CoNPs have moderate antibacterial properties against this bacterium. The CoNPs exhibit moderate antibacterial activity against *E. faecalis*. In all the concentrations used, there was a reduction in

the number of bacterial colony forming units per millilitre over time, which is evidence of bacterial killing. It was observed that the higher concentration of CoNPs leads to a lower value of CFU/mL. However, the standard antibiotic shows a higher decrease in the CFU/mL value within 24, thus more effective in eradicating bacteria. CoNPs demonstrate maximum antibacterial efficacy against *S. mutans* among all the tested NPs. At all concentrations tested, the CFU/mL decreases over time, suggesting that a large amount of bacterial lysis has been achieved. It was observed that as the concentration of CoNPs increased, there was a prominent decline in the number of CFU/mL. The CoNPs at 100 µg/mL possess a similar antibacterial effect to the reference antibiotic, evidencing their possible use as antimicrobial agents against *S. mutans* [26].

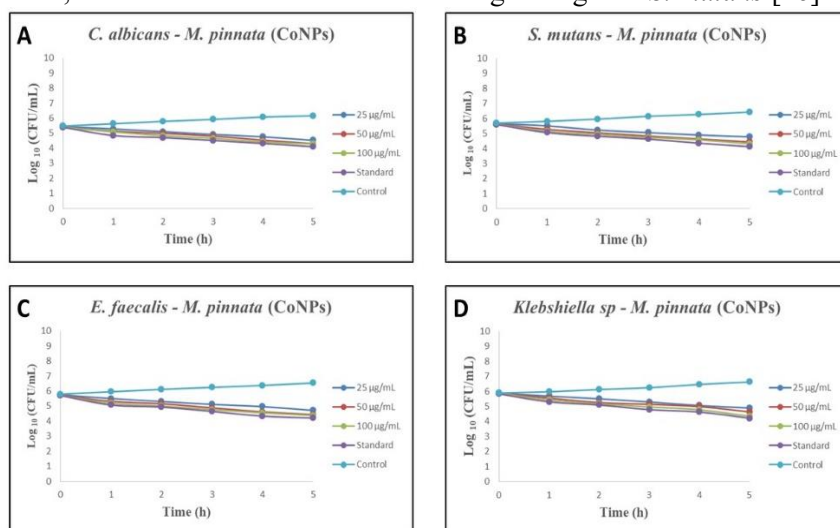


Figure 9. Time Kill Curve Analysis of Cobalt Nanoparticles

Cytotoxicity – Brine Shrimp Lethality Assay (BSLA) of Cobalt Nanoparticles

The Brine Shrimp Lethality Assay (BSLA) assessed the cytotoxicity of CoNPs synthesized from *M. pinnata* leaf extract on brine shrimp nauplii (larvae). After exposing larvae to various CoNPs concentrations for 24 and 48 h (Day 1 and Day 2), the assay measured survival rates. As shown in Figure 10, CoNPs exhibited concentration dependent toxicity, with higher mortality rates corresponding to increased CoNPs concentrations. Time dependent effects

were also noted, as survival rates were generally lower on Day 2 compared to Day 1 at the same concentrations.

At lower concentrations (5, 10 and 20 µg/mL), survival rates remained similar to the control group, indicating minimal toxicity. In contrast, higher concentrations (40 and 80 µg/mL) led to significant decreases in live nauplii, underscoring the toxic effects of prolonged exposure to CoNPs. These results suggest that CoNPs have concentration and time dependent cytotoxic effects on brine shrimp larvae, which could pose environmental

hazards at higher concentrations and with extended exposure. This data offers insight into the cytotoxic impact of CoNPs on *M. pinnata*,

indicating a need for further study on their long term effects in marine ecosystems [27].

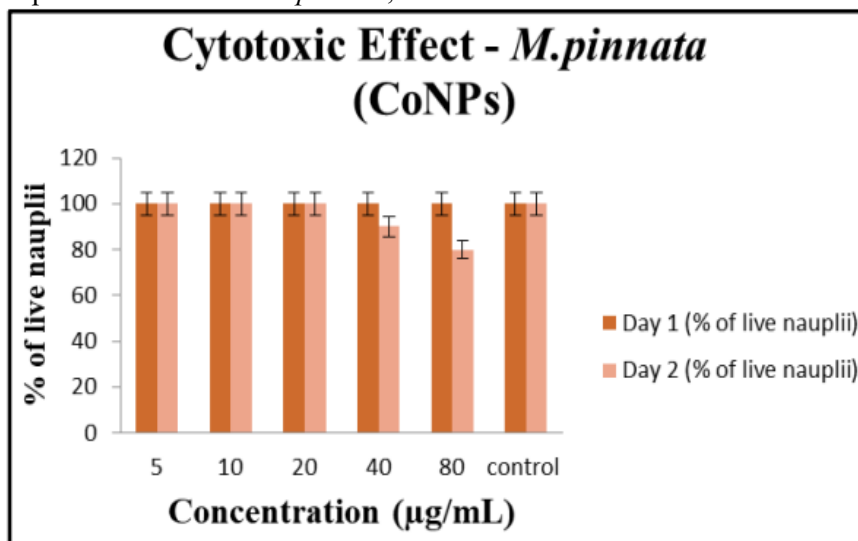


Figure 10. Brine Shrimp Lethality Assay of Cobalt Nanoparticles

Toxicity of Cobalt Nanoparticles in Zebrafish Embryos

The study of the embryonic toxicity of CoNPs in zebrafish embryos offers important information on the possible risks associated with these NPs. The purpose of the experiment assess the effects of various concentrations of

CoNPs on the growth, hatching, and survivability of zebrafish embryos. Photos of zebrafish embryos at different developmental stages are shown in Figure 11 and hatching and survivability rates of zebrafish embryos exposed to different doses of CoNPs (5, 10, 20, 40 and 80 µg/mL) synthesized from leaf extract are shown below.

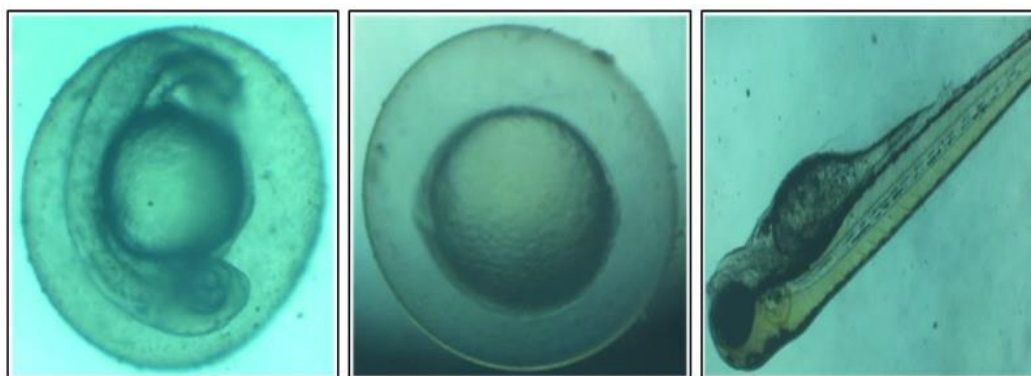


Figure 11. Different Stages of Zebrafish Embryo Development

The control group exhibited a hatching rate that was nearly 100%, suggesting ideal conditions for embryonic development in the absence of CoNPs, according to the graph (Figure 12) showing the hatching rates of zebrafish embryos exposed to various concentrations of CoNPs. Lower quantities of CoNPs (5 and 10 µg/mL) did not significantly

affect hatching rates when compared to the control group but also did not affect viability, indicating that there was little toxicity present at these concentrations. At intermediate quantities (20 and 40 µg/mL), a discernible decrease in hatching rates was noted, suggesting greater toxicity and harmful effects on embryonic development. The hatching

decreased considerably at a high concentration of 80 $\mu\text{g/mL}$, indicating the significant toxicity

of CoNPs at this dose, which significantly affected embryo viability.

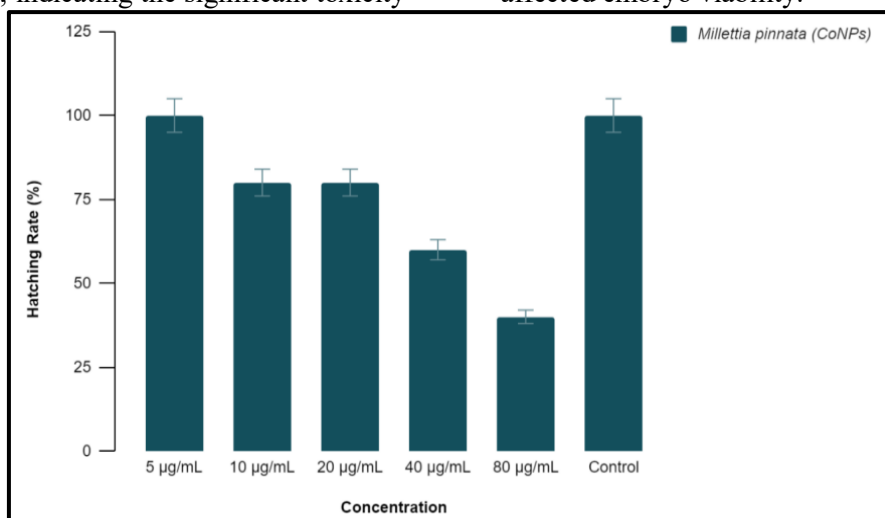


Figure 12. Hatching Rate of Zebrafish Egg Treated with Cobalt Nanoparticles

Figure 13 showing the viability rates of zebrafish embryos post exposure to CoNPs illustrates that the control group again showed near 100% viability, confirming healthy development without CoNPs interference. At low concentrations (5 and 10 $\mu\text{g/mL}$), embryos exhibited high viability rates, similar to the control group, indicating that these CoNPs concentrations are relatively safe. In moderate concentrations there was a decline in viability at 20 and 40 $\mu\text{g/mL}$, corresponding with the hatching rate data, highlighting increased

embryonic mortality due to moderate CoNPs exposure. At high concentrations, the viability rate significantly decreased at 80 $\mu\text{g/mL}$, consistent with the hatching rate data, confirming the high toxicity of CoNPs at this concentration. Under microscopic observation, various malformations were detected in embryos exposed to CoNPs, particularly at higher concentrations. These malformations include developmental delays, physical abnormalities, functional efficiencies etc.

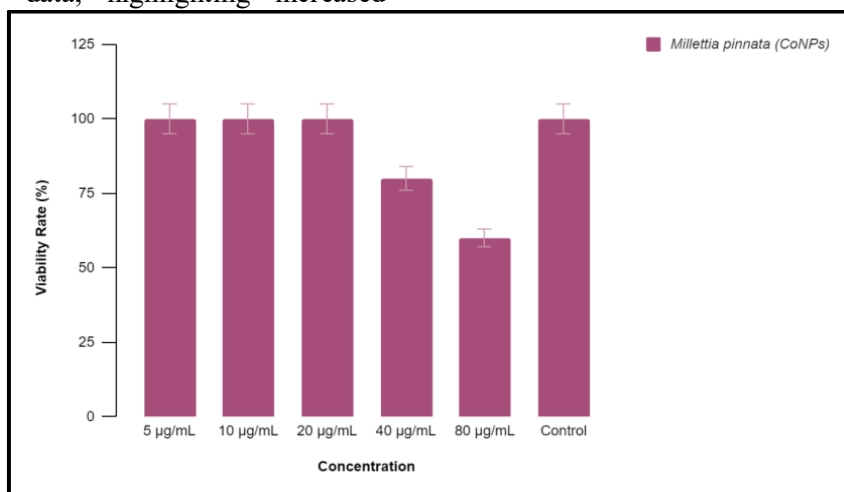


Figure 13. Viability Rate of Zebrafish Egg Treated with Cobalt Nanoparticles

The toxicity study of CoNPs using zebrafish embryos indicated a clear dose dependent relationship between CoNPs concentration and

embryonic development. CoNPs have a high hatching and viability rate and negligible toxicity at lower concentrations (5 and 10

µg/mL). However, as the concentration increases, there is a marked decline in both hatching and viability rates, with significant malformations observed at higher concentrations (20, 40 and 80 µg/mL). This finding highlights the possible problems associated with CoNPs, especially at higher concentrations and emphasizes the necessity of using and disposing of them carefully to reduce biological and environmental concerns. To better understand the underlying causes of CoNPs toxicity and create mitigation plans for their detrimental effects on aquatic life and ecosystems, more research is necessary [28].

Cell Viability - MTT Assay

The cytotoxic effects of CO-MP on osteosarcoma cells. *The in vitro* cytotoxic effect of synthesized CoNPs was evaluated against fibroblast cells at different concentrations (10 - 60 µg/mL) by MTT assay is given in Figure 14. Cells were treated with CO-MP (10 – 60 µg/mL) for 24 h and cell viability was estimated by MTT assay. Data are shown as mean ± SD ($n = 3$). ‘*’ denotes statistical significance ($p < 0.05$) between the control and drug treatment groups. The percentage of cell viability dropped as the concentration of developed CoNPs grew, indicating a dose dependent cytotoxic effect. This indicates that CO-MP exerts cytotoxic effects on osteosarcoma cells [29].

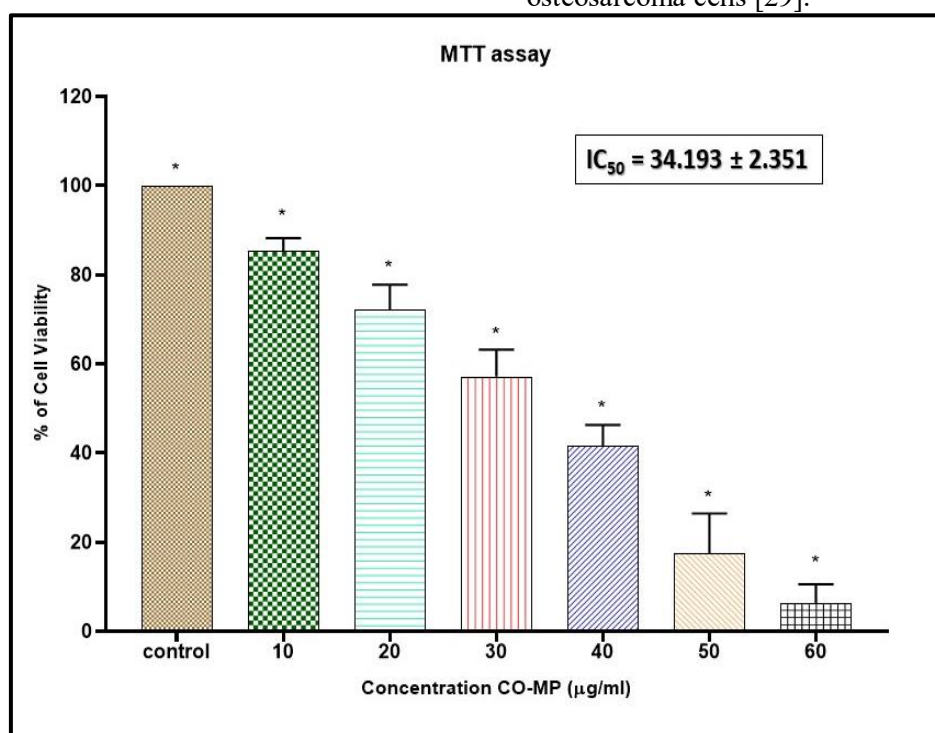


Figure 14. MTT Assay Showing % Viability of Cells Upon Cobalt Nanoparticles Exposure

Effect of Cobalt Nanoparticles on Cell Morphology of Human Osteosarcoma Cells (MG-63)

The effect of CO-MP on human osteosarcoma cells (MG-63) morphology is

shown in Figure 15. Cells were treated with CO-MP (34.19µg/ml) for 24 h and cells were observed under an inverted phase contrast microscope. Following CO-MP treatment, the number of cells shrank and displayed cytoplasmic membrane blebbing [30].

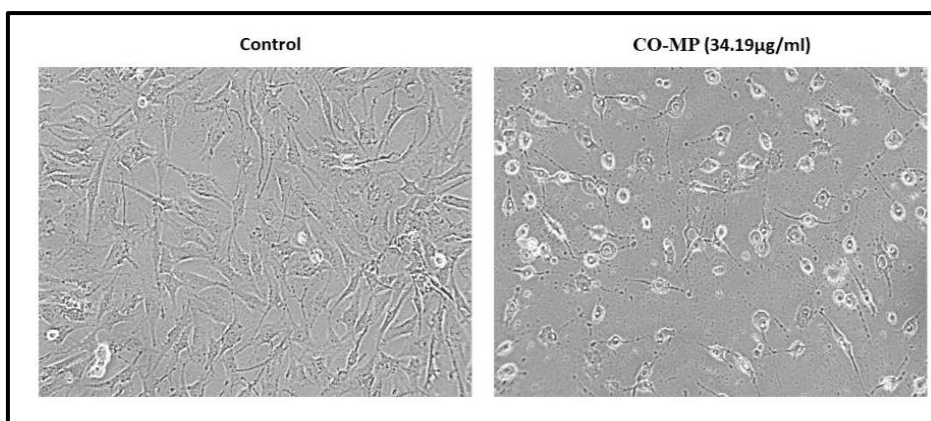


Figure 15. Morphology of Control and Cobalt Nanoparticles Treated Human Osteosarcoma (MG-63) Cells

Detection of Apoptotic Cells in Cobalt Nanoparticles (34.19µg/ml) Treated Osteosarcoma Cells by AO/EtBr Dual Staining

Figure 16 shows the detection of apoptotic cells by AO/EtBr dual labelling in osteosarcoma cells treated with CO-MP (34.19µg/mL). Naringin was applied to human

osteosarcoma cells for a whole day and a control group was also incorporated. The cells were incubated for AO/EtBr dual staining after treatment. An inverted fluorescence microscope was used to obtain images. The cells treated with Naringin extract showed yellow, orange and red colour signals, while control cells were consistently green in colour [31].

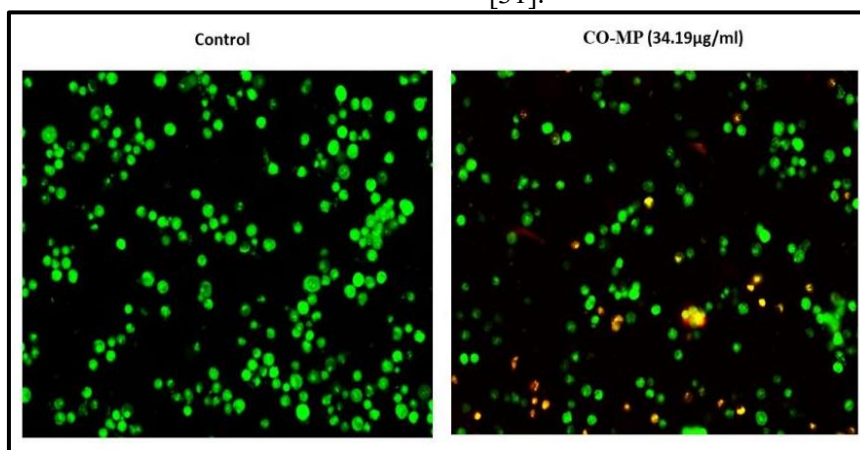


Figure 16. AO/EtBr Dual Staining of Cobalt *Millettia pinnata* Treated Osteosarcoma and Control Cells

Discussion

Nanotechnology has enabled the synthesis of NPs with diverse applications across industry, environmental science and healthcare. Green synthesis, particularly plant based methods, is gaining attention due to its environmentally friendly, cost effective and sustainable advantages. This study explores the synthesis of CoNPs using bioactive compounds from MPL extract, emphasizing an eco friendly approach. The synthesized CoNPs were analyzed through

UV-visible spectrophotometry, FTIR spectroscopy SEM with EDAX for their structural and chemical composition. Additionally, the antibacterial, cytotoxic and embryonic toxicity properties of CoNPs were evaluated.

In UV-Vis analysis, a significant peak at 320 nm was observed, indicating a strong interaction between CoNPs and UV light. The presence of bioactive compounds in MPL likely contributed to a red shift in the UV-Vis spectrum, suggesting a slight alteration in the

nanoparticles electronic environment. This redshift, along with low visible range absorbance and high UV range absorbance, implies that the CoNPs are likely small, monodisperse particles suitable for UV blocking applications. FTIR analysis revealed functional groups such as O-H, C=C, C-H and C-O, corresponding to carboxylic acids, alcohols, ethers and aromatic compounds, which help cap and stabilize CoNPs for improved stability and functionality. SEM images indicated agglomerated particles averaging around 100 nm in size, and EDAX confirmed cobalt along with other elements like oxygen, sodium, chlorine and potassium, signifying successful CoNPs synthesis and stabilization [14, 21].

The synthesized CoNPs displayed antimicrobial activity against *C. albicans*, *S. mutans*, *E. faecalis* and *Klebsiella sp.*, showing notable efficacy against *C. albicans* and *S. mutans*, though a relatively limited impact on *E. faecalis*. Time kill assays supported these findings, suggesting that CoNPs hold promise as antimicrobial agents. Cytotoxic effects were evaluated on osteosarcoma cells via the BSLA and MTT assay. BSLA results indicated a concentration and time dependent toxic effect, with higher concentrations causing significant cell mortality. Additionally, studies on zebrafish embryos demonstrated dose dependent toxicity, with higher doses causing developmental abnormalities [32]. The MTT assay showed dose dependent cytotoxicity on osteosarcoma cells, hinting at potential anticancer applications. AO/EtBr staining further confirmed apoptosis in cancer cells treated with CoNPs, supporting their cytotoxic potential [33].

Comparative studies corroborate the synthesis method used here. For instance, CoNPs synthesized with *Curcuma longa* root extract yielded a UV peak at 345 nm, similar to the 320 nm observed in this study, affirming the effectiveness of the synthesis technique [34]. Likewise, UV visible peaks for nanoparticles

synthesized from *Azadirachta indica* leaf extract within a similar range (250-350 nm), reinforcing the stability and reproducibility of green synthesis methods [35]. Further work has echoed these results, finding consistent UV and FTIR peaks across various studies and validating the synthesis approach [36]. The antibacterial properties of CoNPs against *Klebsiella sp.* and other strains indicate their potential for microbial applications, which aligns with other studies on antimicrobial efficacy.

FTIR analysis identified several functional groups (carboxylic acids, alcohols, ethers and aromatic compounds) that play a role in CoNPs stabilization, echoing previous research on nanoparticle stability facilitated by bioactive compounds [6, 35]. Antibacterial testing showed CoNPs effectiveness against *C. albicans* and *S. mutans*, consistent with findings that reported antibacterial properties against *Staphylococcus aureus* and *Escherichia coli* [14, 37]. The SEM analysis here, which determined an average CoNPs size of 100 nm, also aligns with past studies [38]. The presence of cobalt and oxygen in EDAX results further verifies successful synthesis and composition. The cytotoxicity of CoNPs on osteosarcoma cells, observed in this study, agrees with similar research [39], which highlighted CoNPs anticancer potential. Additionally, dose dependent toxicity in zebrafish embryos correlates with findings on Ag-ZnO nanoparticle toxicity [40], reinforcing the toxicological assessment approach.

In this study, *E. faecalis* appeared less affected by CoNPs compared to findings in earlier research [41]. Overall, the green synthesis of CoNPs from *M. pinnata* leaf extract was effectively demonstrated and supported by both current and prior studies. The synthesized CoNPs show promising applications in multiple fields. In the biomedical sector, their significant antibacterial activity makes them potential candidates for novel antimicrobial agents against resistant

strains such as *C. albicans* and *S. mutans*. The cytotoxic effects observed on osteosarcoma cells suggest a potential role in cancer treatments, presenting a unique avenue for developing anticancer agents. Environmentally, CoNPs can be applied in water treatment by adhering to and decomposing contaminants, thus reducing pollution. In industrial applications, they hold potential in catalytic processes, as FTIR detected surface groups indicate stability and functionality. Additionally, their UV blocking properties make CoNPs suitable for use in UV protective products like paints and sunscreens.

In summary, green synthesized CoNPs from MPL extract show versatile applications, highlighting their utility in antimicrobial treatments, cancer therapies, water treatment, catalysis and UV protective materials. This underscores the value of sustainable, plant based nanoparticle synthesis and provides a foundation for further exploration and development.

References

- [1]. Salem, S. S., Badawy, M. S. E., Al-Askar, A. A., Arishi, A. A., Elkady, F. M., & Hashem, A. H. 2022, Green biosynthesis of selenium nanoparticles using orange peel waste: Characterization, antibacterial and antibiofilm activities against multidrug-resistant bacteria. *Life*, 12(6), 893, <https://doi.org/10.3390/life12060893>
- [2]. Rafique, M., Sadaf, I., Rafique, M. S., & Tahir, M. B. 2017, A review on green synthesis of silver nanoparticles and their applications. *Artificial cells, nanomedicine, and biotechnology*, 45(7), 1272-1291, <https://doi.org/10.1080/21691401.2016.1241792>
- [3]. Keshari, A. K., Srivastava, R., Singh, P., Yadav, V. B., & Nath, G. 2020, Antioxidant and antibacterial activity of silver nanoparticles

Conclusion

The green synthesis of CoNPs using bioactive compounds from *M. pinnata* offers an eco friendly and sustainable approach. Characterization revealed unique physicochemical properties, essential for biological applications. Embryonic toxicology studies showed minimal toxicity, indicating the safety of biomedical use. Additionally, the nanoparticles demonstrated significant anticancer activity, effectively inhibiting cancer cell proliferation. This research highlights the potential of plant derived compounds in nanoparticle synthesis, providing a biocompatible alternative to conventional methods. Future studies should focus on further exploring therapeutic applications and ensuring comprehensive toxicological evaluations for clinical safety.

Conflict of Interest

The authors declare that they have no conflict of interest.

Funding

The authors have no relevant financial or non-financial interests to disclose.

- synthesized by *Cestrum nocturnum*. *Journal of Ayurveda and Integrative Medicine*, 11(1), 37-44, <https://doi.org/10.1016/j.jaim.2017.11.003>
- [4]. Varma, R. S., 2012, Greener approach to nanomaterials and their sustainable applications. *Current Opinion in Chemical Engineering*, 1(2), 123-128, <https://doi.org/10.1016/j.coche.2011.12.002>
 - [5]. Osorio-Cantillo, C., Santiago-Miranda, A. N., Perales-Perez, O., & Xin, Y. 2012, Size-and phase-controlled synthesis of cobalt nanoparticles for potential biomedical applications. *Journal of Applied Physics*, 111(7), 07B324, <http://doi.org/10.1063/1.3676620>
 - [6]. Saeed, S. Y., Mazhar, K., Raees, L., Mukhtiar, A., Khan, F., & Khan, M. 2022, Green synthesis of cobalt oxide nanoparticles using roots extract of *Ziziphys Oxyphylla* Edgew its characterization and

- antibacterial activity. *Materials Research Express*, 9(10), 105001, <https://doi.org/10.1088/2053-1591/ac9350>
- [7]. Safdar, A., Mohamed, H. E. A., Hkiri, K., Muhaymin, A., & Maaza, M. 2023, Green synthesis of cobalt oxide nanoparticles using hyphaene thebaica fruit extract and their photocatalytic application. *Applied Sciences*, 13(16), 9082, <https://doi.org/10.3390/app13169082>
- [8]. Govindasamy, R., Raja, V., Singh, S., Govindarasu, M., Sabura, S., Rekha, K., Rajeswari, V. D., Alharthi, S. S., Vaiyapuri, M., Sudarmani, R., & Jesurani, S. 2022, Green synthesis and characterization of cobalt oxide nanoparticles using Psidium guajava leaves extracts and their photocatalytic and biological activities. *Molecules*, 27(17), 5646, <https://doi.org/10.3390/molecules27175646>
- [9]. Chelliah, P., Wabaidur, S. M., Sharma, H. P., Jweeg, M. J., Majdi, H. S., AL. Kubaisy, M. M. R., Iqbal, A., & Lai, W. C. 2023, Green synthesis and characterizations of cobalt oxide nanoparticles and their coherent photocatalytic and antibacterial investigations. *Water*, 15(5), 910, <https://doi.org/10.3390/w15050910>
- [10]. Jena, R., Rath, D., Rout, S. S., & Kar, D. M. 2020, A review on genus Millettia: Traditional uses, phytochemicals and pharmacological activities. *Saudi Pharmaceutical Journal*, 28(12), 1686-1703, <https://doi.org/10.3390/w15050910>
- [11]. Jeba, D. P., Ramkumar, P., David, A., & Ashli, J., 2022, Synthesis of Green and Pure Copper Oxide Nanoparticles Using Millettia Pinnata Leaf Extract and Their Characterisation. *ECS Transactions*, 107(1), 17335, <https://doi.org/10.1149/10701.17335ecst>
- [12]. Kumar, G., Ghosh, M., & Pandey, D. M., 2019, Method development for optimised green synthesis of gold nanoparticles from Millettia pinnata and their activity in non-small cell lung cancer cell lines. *IET Nanobiotechnology*, 13(6), 626-633, <https://doi.org/10.1049/iet-nbt.2018.5410>
- [13]. Khalil, A. T., Ovais, M., Ullah, I., Ali, M., Shinwari, Z. K., & Maaza, M. 2020, Physical properties, biological applications and biocompatibility studies on biosynthesized single phase cobalt oxide (Co₃O₄) nanoparticles via Sageretia thea (Osbeck.). *Arabian Journal of Chemistry*, 13(1), 606-619, <https://doi.org/10.1016/j.arabjc.2017.07.004>
- [14]. Ali, H., Yadav, Y. K., Ali, D., Kumar, G., & Alarifi, S. 2023, Biosynthesis and characterization of cobalt nanoparticles using combination of different plants and their antimicrobial activity. *Bioscience Reports*, 43(7), BSR20230151, <https://doi.org/10.1042/BSR20230151>
- [15]. Jia, H. R., Zhu, Y. X., Duan, Q. Y., Chen, Z., & Wu, F. G., 2019, Nanomaterials meet zebrafish: Toxicity evaluation and drug delivery applications. *Journal of Controlled Release*, 311, 301-318, <https://doi.org/10.1016/j.jconrel.2019.08.022>
- [16]. Tan, Z., Deng, L., Jiang, Z., Xiang, G., Zhang, G., He, S., Zhang, H., & Wang, Y., 2024, Selenium Nanoparticles Attenuate Cobalt Nanoparticle-Induced Skeletal Muscle Injury: A Study Based on Myoblasts and Zebrafish. *Toxics*, 12(2), 130, <https://doi.org/10.3390/toxics12020130>
- [17]. Ahmad, F., Liu, X., Zhou, Y., & Yao, H. 2015, An in vivo evaluation of acute toxicity of cobalt ferrite (CoFe₂O₄) nanoparticles in larval-embryo Zebrafish (Danio rerio). *Aquatic Toxicology*, 166, 21-28. <https://doi.org/10.1016/j.aquatox.2015.07.003>
- [18]. Ravi, L., Sreenivas, B. A., Kumari, G. S., & Archana, O., 2022, Anticancer cytotoxicity and antifungal abilities of green-synthesized cobalt hydroxide (Co (OH) ₂) nanoparticles using Lantana camara L. *Beni-Suef University Journal of Basic and Applied Sciences*, 11(1), 124, <https://doi.org/10.1186/s43088-022-00304-1>
- [19]. Gayathri, M. K. E., Lakshmi Thangavelu, D. R. S., & Perumal, E. 2023, Green synthesis of cuminal and clove mediated selenium nanoparticles and its anticancer activity against osteosarcoma cell line. *Journal Of Survey in Fisheries Sciences*, 10(1S), 300-311, <https://doi.org/10.17762/sfs.v10i1S.175>
- [20]. Rynthiang, I., Behera, A., Richard, T., & Jothinathan, M. K. D. 2024, An Assessment of the In Vitro Antioxidant Activity of Cobalt Nanoparticles Synthesized from Millettia pinnata,

- Butea monosperma, and Madhuca indica Extracts: A Comparative Study. *Cureus*, 16(4), e59112, <https://doi.org/10.7759/cureus.59112>
- [21]. Ryntathiang, I., Jothinathan, M. K. D., Behera, A., Saravanan, S., & Murugan, R., 2024, Comparative bioactivity analysis of green-synthesized metal (cobalt, copper, and selenium) nanoparticles. *Cureus*, 16(3), e55933, <https://doi.org/10.7759/cureus.55933>
- [22]. Munusamy, T., & Shanmugam, R., 2023, Green synthesis of copper oxide nanoparticles synthesized by Terminalia chebula dried fruit extract: characterization and antibacterial action. *Cureus*, 15(12), e50142, <https://doi.org/10.7759/cureus.50142>
- [23]. Rajeshkumar, S., Santhoshkumar, J., Vanaja, M., Sivaperumal, P., Ponnaniakamideen, M., Ali, D., & Arunachalam, K. 2022, Evaluation of zebrafish toxicology and biomedical potential of aeromonas hydrophila mediated copper sulfide nanoparticles. *Oxidative Medicine and Cellular Longevity*, 2022(1), 7969825, <https://doi.org/10.1155/2022/7969825>
- [24]. Sankar, H. N., Shanmugam, R., & Anandan, J. 2024, Green Synthesis of Euphorbia tirucalli-Mediated Titanium Dioxide Nanoparticles Against Wound Pathogens. *Cureus*, 16(2), e53939, <https://doi.org/10.7759/cureus.53939>
- [25]. Ameena, M., Arumugham, M., Ramalingam, K., Rajeshkumar, S., & Perumal, E. 2023, Cytocompatibility and wound healing activity of chitosan thiocolchicoside lauric acid nanogel in human gingival fibroblast cells. *Cureus*, 15(8), e43727, <https://doi.org/10.7759/cureus.43727>
- [26]. Raja, F. N., Worthington, T., & Martin, R. A. 2023, The antimicrobial efficacy of copper, cobalt, zinc and silver nanoparticles: alone and in combination. *Biomedical Materials*, 18(4), 045003, <https://doi.org/10.1088/1748-605X/acd03f>
- [27]. Palaniappan, P., Thamaynathi, S., Maharifa, H. N. S., & Ramesh, R., 2021, Green Synthesis of Copper (Cu) Nanoparticles Using Marine Brown Algae Turbinaria Ornata and Its Brine Shrimp Lethality Bioassay. *International Journal of Nanotechnology and Nanomedicine*, 6(2), 35-40, <https://dx.doi.org/10.33140/IJNN>
- [28]. Mutalik, C., Nivedita, Sneka, C., Krisnawati, D. I., Yougbaré, S., Hsu, C. C., & Kuo, T. R. 2024, Zebrafish Insights into Nanomaterial Toxicity: A Focused Exploration on Metallic, Metal Oxide, Semiconductor, and Mixed-Metal Nanoparticles. *International Journal of Molecular Sciences*, 25(3), 1926, <https://doi.org/10.3390/ijms25031926>
- [29]. Kumar, R., Huda, M. N., Habib, A., Nafiujjaman, M., Woo, H. J., Kim, T., & Nurunnabi, M., 2023, Carbon Coated Iron–Cobalt Nanoparticles for Magnetic Particle Imaging. *ACS Applied Bio Materials*, 6(8), 3257-3265, <https://doi.org/10.1021/acsabm.3c00354>
- [30]. Shashiraj, K. N., Hugar, A., Kumar, R. S., Rudrappa, M., Bhat, M. P., Almansour, A. I., Perumal, K., & Nayaka, S., 2023, Exploring the antimicrobial, anticancer, and apoptosis inducing ability of biofabricated silver nanoparticles using Lagerstroemia speciosa flower buds against the Human Osteosarcoma (MG-63) cell line via flow cytometry. *Bioengineering*, 10(7), 821, <https://doi.org/10.3390/bioengineering10070821>
- [31]. Berehu, H. M., & Patnaik, S., 2024, Biogenic Zinc Oxide Nanoparticles synthesized from Tinospora Cordifolia induce oxidative stress, mitochondrial damage and apoptosis in Colorectal Cancer. *Nanotheranostics*, 8(3), 312, <https://doi.org/10.7150/ntno.84995>
- [32]. Varghese, R. M., Kumar, A., & Shanmugam, R., 2024, Cytotoxicity and characterization of zinc oxide and silver nanoparticles synthesized using Ocimum tenuiflorum and Ocimum gratissimum herbal formulation. *Cureus*, 16(2), e53481, <https://doi.org/10.7759/cureus.53481>
- [33]. Waris, A., Din, M., Ali, A., Afridi, S., Baset, A., Khan, A. U., & Ali, M., 2021. Green fabrication of Co and Co₃O₄ nanoparticles and their biomedical applications: A review. *Open Life Sciences*, 16(1), 14-30, <https://doi.org/10.1515/biol-2021-0003>
- [34]. Shanmuganathan, R., Sathiyavimal, S., Le, Q. H., Al-Ansari, M. M., Al-Humaid, L. A., Jhanani, G. K., Lee, J., & Barathi, S., 2023, Green synthesized cobalt oxide nanoparticles using Curcuma longa for anti-oxidant, antimicrobial, dye degradation and anti-cancer property. *Environmental Research*, 236,

- 116747,
<https://doi.org/10.1016/j.envres.2023.116747>
- [35]. Singh, D., Sharma, P., Pant, S., Dave, V., Sharma, R., Yadav, R., Prakash, A., & Kuila, A. 2024, Ecofriendly fabrication of cobalt nanoparticles using *Azadirachta indica* (neem) for effective inhibition of *Candida*-like fungal infection in medicated nano-coated textile. *Environmental Science and Pollution Research*, 31(34), 46575-46590, <http://dx.doi.org/10.1007/s11356-023-28061-3>
- [36]. Imtiyaz, A., Singh, A., & Gaur, R., 2024, Comparative Analysis and Applications of Green Synthesized Cobalt Oxide (Co₃O₄) Nanoparticles: A Systematic Review. *BioNanoScience*, 14, 1-19, <http://dx.doi.org/10.1007/s12668-024-01452-7>
- [37]. Anupong, W., On-Uma, R., Jutamas, K., Joshi, D., Salmen, S. H., Alahmadi, T. A., & Jhanani, G.K. 2023, Cobalt nanoparticles synthesizing potential of orange peel aqueous extract and their antimicrobial and antioxidant activity. *Environmental Research*, 216, 114594. <https://doi.org/10.1016/j.envres.2022.114594>
- [38]. Bhutekar, P. G., Kshirsagar, A. K., Bankar, S. S., & Mirgane, S. R. 2023, Green Synthesis and Characterization of Iron and Cobalt Oxide Nanoparticles Using *Phaseolus Lunatus* Flower Extract. *Journal for ReAttach Therapy and Developmental Diversities*, 6(9s), 1951-1956, <https://doi.org/10.53555/jrtdd.v6i9s.2813>
- [39]. Sharifi, E., Reisi, F., Yousefiasl, S., Elahian, F., Barjui, S. P., Sartorius, R., Fattahi, N., Zare, E. N., Rabiee, N., Gazi, E. P., & Paiva-Santos, A. C., 2023, Chitosan decorated cobalt zinc ferrite nanoferrofluid composites for potential cancer hyperthermia therapy: anti-cancer activity, genotoxicity, and immunotoxicity evaluation. *Advanced Composites and Hybrid Materials*, 6(6), 191, <http://dx.doi.org/10.1007/s42114-023-00768-4>
- [40]. Anbarasu, M., Martin, T. M., Priya, P., Sivamurugan, V., Kumar, M. S. K., Shaik, M. R., Kari, Z.A., & Guru, A. 2024, Assessing the impact of Ag-ZnO nanoparticle on the induction of oxidative stress, hematological, and molecular changes in zebrafish (*Danio rerio*) and McCoy fibroblast cell lines. *Aquaculture International*, 32(4), 5373-5392, <http://dx.doi.org/10.1007/s10499-024-01611-3>
- [41]. Kannan, V. D., Jaisankar, A., Rajendran, V., Ahmed, M. Z., Alqahtani, A. S., Kazmi, S., Madav, E., Sampath, S., & Asaithambi, P. 2024, Ecofriendly bio-synthesis and spectral characterization of copper nanoparticles using fruit extract of *Petalium murex* L.: in vitro evaluation of antimicrobial, antioxidant and anticancer activities on human lung cancer A549 cell line. *Materials Technology*, 39(1), 2286818, <https://doi.org/10.1080/10667857.2023.2286818>